X-ray reflectivity of the Cu(110) surface

G. Helgesen and Doon Gibbs
Department of Physics, Brookhaven National Laboratory, Upton, New York 11973

A. P. Baddorf and D. M. Zehner
Solid State Division, Oak Ridge National Laboratory, Oak Ridge, Tennessee 37831

S. G. J. Mochrie
Department of Physics, Massachusetts Institute of Technology, Cambridge, Massachusetts 02139
(Received 12 May 1993)

The specular reflectivity from the (110) surface of a Cu single crystal has been measured for temperatures between 300 and 1100 K. At lower temperatures, the reflectivity is well described by a model which yields a contraction of the spacing between the first and the second surface layers by 8% relative to the bulk layer separation. The fits also show large surface-normal vibrational amplitudes within the first few atomic layers. The line shape of the scattering transverse to the specular direction has two components below 1000 K, and evolves with increasing temperature. However, our data do not preclude the existence of a surface-roughening transition.

I. INTRODUCTION

It is generally expected that the surface of a crystal will become more disordered as the temperature is raised toward the bulk melting point. A variety of different disordering phenomena have been proposed theoretically, including roughening, which involves a divergence in the variance of the surface position, and premelting, which is the loss of translational order within the surface or near-surface layers. Above the roughening temperature, the surface height-height correlation function shows a logarithmic divergence with distance across the surface,[1] leading to a power-law description of the diffracted intensity as a function of the in-plane component $Q_{\parallel}$ of the scattering vector.[2] Faceting, wherein a surface slightly misaligned or "miscut" from a high-symmetry direction phase separates into regions of low step density and regions of high step density, is also possible. Finally, surface atoms may show enhanced vibrational amplitudes compared to the bulk. A focus of current theoretical and experimental interest is to determine the extent to which these concepts describe the (110) surfaces of face-centered-cubic metals.[3] In spite of this effort, a general understanding has not yet emerged.

Apparent roughening transitions have been observed by high-resolution low-energy electron diffraction for the Pb(110) (Ref. 4) and Ni(110) (Ref. 5) surfaces. The situation for Ag(110) surfaces, however, is unclear with reports alternatively of roughening[6] and faceting[7] transformations, possibly with step pinning by impurities playing an important role.[8] X-ray-scattering experiments have given evidence for roughening transitions below the bulk melting temperature T_M for the (113) surfaces of Cu (Ref. 9) and Ni,[9] and also for the hexagonally reconstructed Pt(001) surface.[10] The reported roughening temperatures vary from $0.45T_M$ for Ni(113) (Ref. 2) and Cu(113),[9] to $0.89T_M$ for Pt(001).[10] For the (110) surfaces of Pb and Ni, roughening is observed near $0.69T_M$ and $0.75T_M$, respectively.[4,5] Surface premelting has been observed experimentally for the Pb(110) surface 40 K below T_M by ion scattering.[11]

Much effort has been directed toward an understanding of the Cu(110) surface. The Cu(110) surface has been observed to disorder at high temperatures by He beam diffraction[12] and low-energy ion scattering.[13] On the basis of x-ray-scattering experiments,[14] it was proposed that the Cu(110) surface has a roughening transition at about 900 K (which corresponds to $\approx 0.66T_M$). However, later x-ray experiments[15] showed that surface miscuts by 0.8° and 0.2° of these crystals lead to reversible faceting at temperatures below 900 K, thereby explaining the observations which had been attributed to roughening of the (110) facet in Ref. 14. Subsequently, He-scattering experiments[16] yielded no evidence of a roughening transition on the basis of the absence of a change in the scattering line shape. Instead, the behavior of the Cu(110) surface observed above 500 K was attributed to an anomalously large anharmonicity of the atomic vibrations at the surface. The results from a wide range of other techniques including He-atom scattering,[17] mirror electron microscope low-energy electron diffraction,[18] and impact-collision ion-scattering spectroscopy[19] have also been interpreted in terms of large, anharmonic surface vibrations. Large surface anharmonicity has been experimentally observed by high-resolution electron-energy-loss spectroscopy.[20] Computer simulations[21–23] have also indicated that the surface vibrations are anharmonic. More recent molecular-dynamics and Monte Carlo computer simulations[24] have suggested that surface disordering proceeds in a stepwise fashion with a roughening transition near 1000 K and a premelting of the surface about 50 K below the bulk melting temperature. Very re-

0163-1829/93/48(20)/15320(6)/$06.00

cently, Kern[25] has stated that new He-scattering measurements reveal a roughening transition at $T_R = 1080$ K$=0.8T_M$, but the data have yet to be published.

In this paper we report measurements of the x-ray specular reflectivity of the Cu(110) surface for temperature between 300 and 1000 K. X-ray scattering is one of the few structural probes which is sensitive to the structure of more than a few surface layers. Moreover, since the x-ray reflectivity from both ideally terminated and reconstructed surfaces can be easily calculated,[26] it is possible in principle to find both the atomic displacements and the root-mean-square (rms) vibrational amplitudes (or the Debye Waller factors) of the different layers. Our data display a clear evolution with temperature. First, the integrated intensity of the specular reflectivity decreases, indicating that the normal displacement amplitudes of the surface layers increase with temperature. In addition, we observe that the line shapes of scans transverse to the surface-normal direction exhibit two components, one sharp (resolution limited) and the other diffuse. For increasing temperatures, the intensity of the sharp component decreases, and is absent above 1000 K. This suggests that the surface is stepped, and possibly rough above 1000 K over areas comparable in size to the resolution area ($\approx$2000 Å). However, our data do not establish a specific roughening transition, above which there is a logarithmic divergence of the height-height correlation function.

II. THE EXPERIMENT

The x-ray-scattering experiments were performed at beamline X22C at the National Synchrotron Light Source, Brookhaven National Laboratory. The sample ($13\times13\times3$ mm^3) was held in an ultrahigh vacuum chamber with a pressure less than 5×10^{-10} Torr. The orientation of the surface normal was parallel to the [110] direction to within about 0.1°. Two azimuthal orientations were studied, one with the [001] direction in the scattering plane and one with the [1$\bar{1}$0] direction in the scattering plane. The size of the illuminated sample area was typically limited by slits in front of the sample to 1×3 mm^2. The resolution of the spectrometer for a photon energy of 8.1 keV ($\lambda=1.53$ Å) was 3×10^{-3} Å^{-1}, and 2×10^{-3} Å^{-1} in the scattering plane parallel to and perpendicular to the surface normal, respectively, and about 3×10^{-2} Å^{-1} perpendicular to the scattering plane at the (220) reflection.

Prior to the x-ray experiments, the sample was subject to extensive Ar sputtering and high-temperature annealing cycles to clean the surface. This annealing improved the bulk mosaic, finally leading to a value of 0.03° at the (220) reflection. During the x-ray-scattering measurements, the sample surface was also cleaned by Ar-ion sputtering and annealing at 800 K for 10–30 min before measurements at each new temperature. The sample was heated by electron bombardment from a filament located behind it and the temperature was monitored by a (WRe5%–WRe26%) thermocouple. We did experiments at temperatures up to about 100 K below the bulk melting point, but the observed reflectivity was not reproducible at the highest temperatures, and is not reported here.

Before and after some of the measurements the surface cleanliness was measured by Auger-electron spectroscopy. Unfortunately, the Auger spectroscopy revealed detectable amounts of sulfur on the surface whenever the sample was held at temperatures above 1000 K for more than about a half hour. Two months of annealing the sample in a hydrogen atmosphere did not significantly reduce the amount of sulfur. Sulfur contamination at high temperatures has also been reported in earlier experiments.[18,19] Nevertheless, at lower temperatures no detectable contamination of the surface could be observed by Auger spectroscopy during the experiments.

III. RESULTS AND DISCUSSION

Transverse scans (θ scans) through the specular rod were taken for a range of values of the surface-normal scattering wave vector $\mathbf{Q}_\perp=(Ha^*,Ha^*,0)$ with H between 0.2 and 2.7. Here, $a^*=2\pi/a$, with lattice constant $a=3.615$ Å at room temperature. The measurements were carried out for many different temperatures between 300 and 1000 K. A few of these scans taken at room temperature are shown in Fig. 1. Note the decrease in intensity near $H=1.0$. The increase in the background near $H=2$ is caused by thermal diffuse scattering from the bulk. In order to calculate the integrated intensity (reflectivity), it was found necessary to fit these data to a two-component line shape. This is particularly clear for the data at small $\mathbf{Q}_\perp$ in Fig. 1, and is highlighted in Fig. 2.

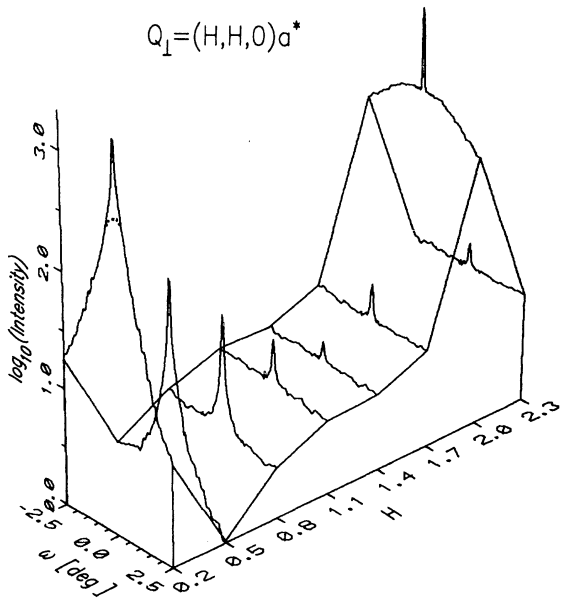

FIG. 1. Transverse scans through the specular rod at room temperature for some values of the surface-normal scattering wave vector $\mathbf{Q}_\perp=(Ha^*,Ha^*,0)$. Here, $\omega=\theta-(2\theta)/2$. The large background in the scan near the (2,2,0) Bragg peak is caused by the thermal diffuse scattering. Note the broad component of the peak at small $\mathbf{Q}_\perp$ as indicated by the dotted line for $H=0.2$ and also shown in Fig. 2. Intensity is in arbitrary units.

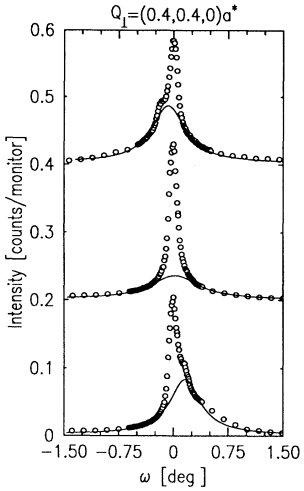

FIG. 2. Scans along the [1$\bar{1}$0] direction through the specular rod at three different positions on the sample surface. The translation of the crystal was parallel to the [1$\bar{1}$0] direction. The middle, symmetric scan is from the center of the sample, while the upper and lower scans are near two opposite edges. Circles show the measured intensity, and the solid lines show the broad component obtained in fits of the data to a two-component line shape. (The scans are shifted vertically for clarity.)

We tried several combinations of Gaussians, Lorentzians, and Lorentzian-squared curves. The best fits were obtained using a combination of a broad Lorentzian [full width at half maximum (FWHM)=0.6±0.1°] and a sharper, resolution-limited Lorentzian-squared (FWHM=0.17±0.02°). The in-plane characteristic length ξ corresponding to the inverse of the half-width at half maximum of the sharp peak (5×10^{-4} Å^{-1} at $H=0.2$) is $\xi\approx2000$ Å. For $H>1.1$, the peaks were well described by only a single Lorentzian-squared component. The widths of the two components were roughly independent of $\mathbf{Q}_\perp$. Although the data required two components to be fitted at all $H<1.0$ and for all temperatures, we do not attribute any particular significance to the forms of the fitted line shapes (Lorentzian vs Lorentzian squared) due to limited statistics. Consequently, we are unable to draw any conclusions concerning the possible divergence of the height-height correlation function of the surface.

It is important to note that by moving the illuminated area across the sample at small scattering angles (small $\mathbf{Q}_\perp$), the relative positions of the broad and narrow components shifted. When the beam was moved parallel to the scattering plane across the sample, the broad component shifted from being at one side of the narrow component to being at the other side, as shown in Fig. 2. The maximum relative displacement of the two components was about 0.15°, and near the center of the sample the displacement was less than 0.07°. Since the sharp component corresponds to specular reflection from the crystallographic (110) oriented surface, we infer that this component corresponds to the scattering from smooth (110) facets. The measured width of the sharp component then implies that the (110) facets are at least 2000 Å in size. According to this interpretation, the broad component arises from stepped regions on the surface. Its position depends on the local average surface-normal direction. The interpretation of the displacement of the broad component shown in Fig. 2 is that the macroscopic surface profile parallel to the (001) planes of the crystal is slightly convex.

The specular reflectivity for three different temperatures is shown in Fig. 3. The solid lines in this figure show the best fits to a model for the reflectivity. In general, the specular reflectivity R is given by the expression[26]

$$R=\frac{P4\pi^2r_0^2}{\Gamma^2k^2\sin^2\theta}|T(\theta)|^4|F(Q_\perp)|^2\times\left|\sum_{n=0}^{\infty}\rho_n e^{-iz_nQ_\perp}e^{-W_n(Q_\perp)}\right|^2, \quad (1)$$

where $F(Q_\perp)$ is the form factor, $W_n(Q_\perp)$ is the Debye-Waller factor, z_n is the position of the nth layer with relative density ρ_n, $k=2\pi/\lambda$, r_0 is the Thomson radius of the electron, Γ is the area per atom in each plane, P is a polarization factor, and $T(\theta)$ is the Fresnel transmission coefficient.[27] At 300 K the separation d between the (110) layers in the bulk is $d=a/2\sqrt{2}=1.28$ Å. Then, $z_n=(1-n+\varepsilon_n)d$, where ε_n is the relative displacement of layer n relative to its position in an ideally terminated crystal, and the distance between layer n and layer $n+1$ is $d_{n,n+1}=(1+\varepsilon_n-\varepsilon_{n+1})d$. We have shown the reflectivity for an ideally terminated surface at 300 K as a dashed line in Fig. 3(a). Our model allows variation of

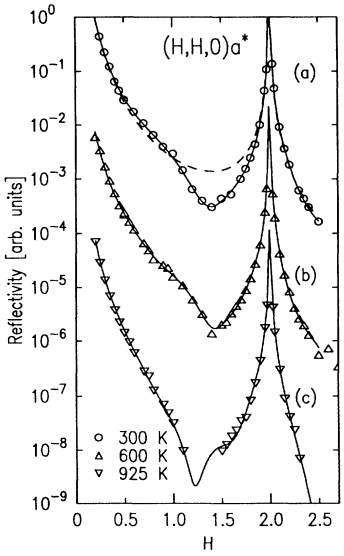

FIG. 3. X-ray specular reflectivity for the Cu(110) surface at (a) 300, (b) 600, and (c) 925 K. The curves are shifted for clarity. The solid lines are best fits to a reflectivity model for the surface as discussed in the text. The dashed line in (a) shows the specular reflectivity of an ideally terminated surface at 300 K.

the parameters for four layers beneath the surface. The perpendicular positions z_n ($n=1,2,3,4$) of the layers were variables to be fitted together with the root-mean-square (rms) amplitudes σ_n of the atomic vibrations perpendicular to the surface in the Debye-Waller factor $W_n(Q_\perp)=\frac{1}{2}\sigma_n^2 Q_\perp^2$. For the Debye-Waller factor of the bulk, we used the values found in the measurements by Martin and O'Connor,[28] which show anharmonicity of bulk vibrations for $T>400$ K. The densities ρ_n were kept fixed at their bulk values. To avoid an inappropriate biasing of the fits by low reflectivity points with large error bars, these points were removed, and the data were refitted. However, this gave only small changes in the best-fit parameters.

The measured reflectivity in Fig. 3 decreases from its value near $H=0.2$ until about $H=1$ (consistent with Fresnel's law), and rises again near the Bragg peak ($H=2$). The main discrepancy of the measured reflectivity from that expected for an ideally terminated surface [dashed line in Fig. 3(a)] occurs near $H=1.3$. The fits show that the large decrease in reflectivity at $T=300$ K near $H=1.3$ in Fig. 3(a) is caused by a contraction of the top surface layer by $|\varepsilon_1|=(6.0\pm0.5)\%$ relative to the position of the first layer in an ideally terminated surface. The small shoulder seen at $H=0.8$ can be related to an expansion of the second layer by $\varepsilon_2=(1.8\pm0.5)\%$. These results correspond to an 8% reduction of the distance d_{12} between the two top layers. The best fits also show a small contraction of the third layer by less than 1%. The values of the contractions are in agreement with earlier measurements by low-energy electron diffraction (LEED),[29–31] high-energy ion scattering (HEIS),[29,32] and medium-energy ion scattering (MEIS),[33] which show changes of the layer separations d_{12} (first-second layer) and d_{23} (second-third layer) by -8.5% and $+2.3\%$ (from LEED), -5.3% and $+3.3\%$ (from HEIS), and -7.5% and $+2.5\%$ (from MEIS), respectively.

Except for a decrease in the reflectivity with increasing temperatures, the Q dependence of the line shapes are qualitatively similar between 300 and 925 K. Figure 4(a) shows the temperature dependence of the top-layer contraction obtained from fits to data like that shown in Fig. 3. Between 300 and 700 K the contraction of the top layer changes little, but at higher temperatures our fits suggest that the contraction decreases and at 925 K it is reduced to about 3%. However, as seen in Fig. 4(a) the uncertainty in the values of ε_1 at high temperatures is relatively large. The main reason is that there is a strong correlation in the fits between the values of ε_1 and the vibrational amplitude σ_1. The change in ε_1 cannot, therefore, be interpreted as a definitive proof for a reduction of the top-layer contraction with increasing temperature. However, recent computer simulations using effective-medium theory[24] show a similar reduction in the first interlayer spacing d_{12} with temperature, although the contraction of d_{12} at room temperature in the simulations is only about half of our value. Moreover, such an expansion is expected for anharmonic vibrations. The change with temperature of the positions of the second and third layers does not show a clear trend, but the shifts of the second- and third-layer positions relative to the corresponding bulk layers, $|\varepsilon_2|$ and $|\varepsilon_3|$, are less than 2% and 1%, respectively, at all the higher temperatures.

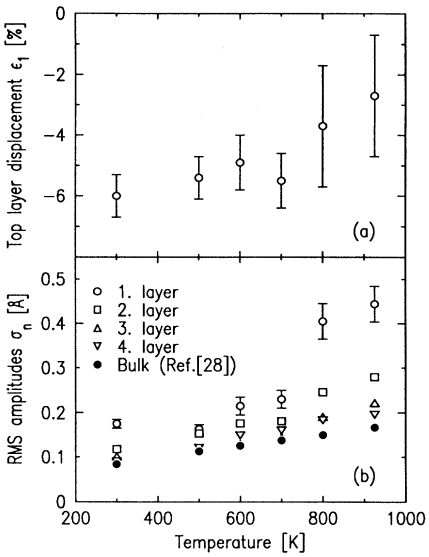

FIG. 4. (a) The relative displacement ε_1 from the bulk-terminated position of the surface top layer vs temperature found in the fits of the specular reflectivity. (b) The rms surface-normal vibrational amplitudes of the four top layers of the (110) surface. The filled circles show the vibrational amplitudes of the bulk from Ref. 28.

The most important factor in reducing the surface reflectivity in the region near $H=1.3$ at higher temperatures is the rapid increase in the Debye-Waller factor for the top layers of the crystal. The rms surface-normal vibrational amplitudes σ_n of the first few layers calculated from the fitted Debye-Waller factors are shown in Fig. 4(b) together with the bulk values.[28] At room temperature the value of σ_1 for the top layer is almost twice the bulk value, and the values for the second and third layers are also slightly increased. As the temperature increases, all of the rms amplitudes σ_n increase faster than the bulk value σ_{bulk}. There is a very large increase in σ_1 between 700 and 800 K, and at 925 K σ_1 is almost three times the bulk value.

The rms vibrational amplitudes shown in Fig. 4(b) are in relatively good agreement with the values found in Ref. 18 from LEED studies, but the value of σ_1 at high temperatures is about 30% larger than that reported in other experiments.[17,19] Our results are also in good agreement with computer simulations,[21,24] which show a large increase in the amplitude of the surface-normal vibrations above 600–700 K. It is interesting to note that using the Lindemann criterion,[34] which predicts that melting will occur when the vibrational amplitude is about 10% of the interatomic spacing (here $\sigma_n>0.26$ Å), the first layer should be melted at 800 K, and the second layer at 900 K. Although the criterion should not be used for separate layers, it gives a clear indication of the unusually large thermal vibrations of the top layers in the Cu(110) surface at temperatures above 600–700 K. Un-

fortunately, the presence of sulfur contamination on the surface which occurred above 1000 K has prevented meaningful analysis of the measured reflectivity closer to the bulk melting temperature.

It should be noted that modifications of the reflectivity model used in the fits change the temperature variations for the surface parameters shown in Fig. 4. However, by adding more free fitting variables, such as the density ρ_1 of the top layer, or the density of atoms in an additional adatom layer, the fits were not significantly improved. Such modifications of the model changed, in particular, the values of σ_1 and ε_1. Since the change in the quality of the fits was not large enough to distinguish between the various modifications of the model, the results presented in Figs. 3 and 4 were obtained by using the simplest possible model. From our testing of different variations of this basic model, it can be concluded that the addition of a partly filled adatom layer has a similar effect on the specular reflectivity as an expansion of the top-layer spacing ε_1, accompanied by an increase in the Debye-Waller rms amplitude σ_1.

Finally, we discuss the temperature dependence of the transverse line shapes. Transverse scans taken as a function of temperature at $H=0.4$ are shown in Fig. 5(a). These data have been fitted to the sum of narrow and broad components, as discussed earlier in the text. As may be seen, the intensity of the narrow component decreases dramatically with increasing temperature with respect to that of the broad component underneath. These results are quantified in Fig. 5(b), which shows the total integrated intensity versus temperature, together with the integrated intensities of the sharp and broad components separately. It is clear that the decrease in total intensity is accounted for by the gradual disappearance of the sharp component. The width of the narrow component of the peak is relatively independent of the temperature. A similar behavior is found at larger $\mathbf{Q}_\perp$.

In our view, the simplest interpretation of the two-component line shapes measured in transverse scans of the specular reflectivity is in terms of surface faceting, in which one domain is smooth and aligned to the crystallographic [110] direction, while the other supports a high density of steps. If there were only a single domain type at this surface, oriented at the macroscopic miscut of 0.07° away from the [110] direction, then (assuming monatomic steps), there would be one step for every 400 Cu atoms along the $[1\bar{1}0]$ direction. This corresponds to an average step separation of about 1000 Å, which is one-half of the measured characteristic length ξ, and would give only a single component in a transverse scan. A faceted surface, on the other hand, is consistent with earlier reflectivity experiments on Cu(110) surfaces miscut by 0.2° and 0.8°, respectively.[15] In those studies, the surfaces were found to facet below ≈ 520 K. Also similar to the present case, a sharp peak aligned to the [110] direction disappeared above 900 K in those studies, leaving only a broad peak related to the average surface miscut. The disappearance of the sharp component (and the slight increase in the intensity of the broad component) seen in Fig. 5(b) probably signals the proliferation of steps across the formerly smooth (110) facets. Unfortunately, it is impossible to deduce the microscopic surface morphology from our data, for example, to reliably extract the average step-step separation. Nor is it possible to characterize the long-ranged behavior of the height-height correlation function, as is necessary in order to convincingly distinguish between a rough surface with a divergent variance of the surface height, and a step-disordered flat surface.[3]

IV. CONCLUSIONS

We have measured the specular reflectivity of a Cu(110) surface for temperatures between 300 and 1000 K. For small values of $\mathbf{Q}_\perp$ the line shape of the scattering is best described as a sum of a narrow, resolution-limited component and a broader component. At larger $\mathbf{Q}_\perp$ only the narrow peak is observed. Fits to a simple model for the surface reflectivity show that at room temperature the distance between the first and second surface layers is contracted by about 8%. This contraction decreases as the temperature increases. The gradual decrease in the x-ray reflectivity above 600–700 K shows that the surface becomes more disordered at higher temperatures, consistent with the disappearance of the smooth (110) facets. This is also indicated by the large increase in the fitted rms amplitude σ_1 of the surface-normal vibrations of the top layer. The surface-normal vibrational amplitudes for the second and third layers are also much larger than the bulk values. X-ray specular reflectivity measurements on macroscopically flatter single-crystal surfaces of higher purity may give further insight into the behavior of the (110) surface of copper just below its melting temperature.

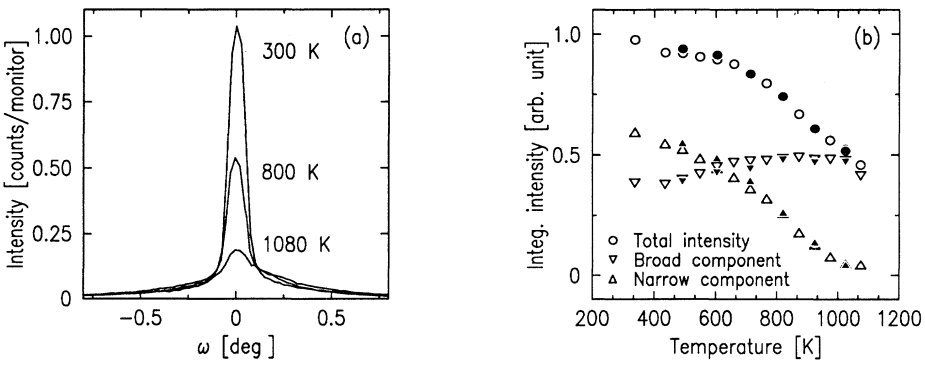

FIG. 5. Specular reflectivity at $\mathbf{Q}_\perp=(0.4a^*,0.4a^*,0)$. (a) Transverse scans for three different temperatures $[\omega=\theta-(2\theta)/2]$. (b) The total integrated intensity (upper curve) and the integrated intensity of the narrow and broad components of the peak as a function of temperature. The open (filled) symbols are for decreasing (increasing) temperatures.

ACKNOWLEDGMENTS

Work at Brookhaven was supported by the U.S. Department of Energy under Contract No. DE-AC02-76CH00016. Work performed at MIT was supported by the NSF Grant No. DMR-9119675. Work at ORNL was sponsored by the U.S. DOE under Contract No. DE-AC02-840R21400, with Martin Marietta Energy Systems Inc. G.H. would like to acknowledge the Research Council of Norway for partial support.

[1]For a review, see J.D. Weeks, in *Ordering in Strongly Fluctuating Condensed Matter Systems,* edited by T. Riste (Plenum, New York, 1980), p. 293.

[2]I. K. Robinson, E. H. Conrad, and D. S. Reed, J. Phys. (France) **51**, 103 (1990).

[3]See, e.g., M. den Nijs, Phys. Rev. B **46**, 10 386 (1992).

[4]H.-N. Yang, T.-M. Lu, and G.-C. Wang, Phys. Rev. Lett. **63**, 1621 (1989).

[5]Y. Cao and E. H. Conrad, Phys. Rev. Lett. **64**, 447 (1990).

[6]G. A. Held, J. L. Jordan-Sweet, P. M. Horn, A. Mak, and R. J. Birgeneau, Phys. Rev. Lett. **59**, 2075 (1987).

[7]I. K. Robinson, E. Vlieg, H. Hornis, and E. H. Conrad, Phys. Rev. Lett. **67**, 1890 (1991).

[8]G. A. Held, D. M. Goodstein, R. M. Feenstra, M. J. Ramstad, D. Y. Noh, and R. J. Birgeneau, Phys. Rev. B **48**, 8458 (1993).

[9]K. S. Liang, E. B. Sirota, K. L. D'Amico, G. J. Hughes, and S. K. Sinha, Phys. Rev. Lett. **59**, 2247 (1987).

[10]D. L. Abernathy, S. G. J. Mochrie, D. M. Zehner, G. Grübel, and Doon Gibbs, Phys. Rev. Lett. **69**, 941 (1992).

[11]J. W. M. Frenken and J. F. van der Veen, Phys. Rev. Lett. **54**, 134 (1985).

[12]D. Gorse and J. Lapujoulade, Surf. Sci. **162**, 847 (1985).

[13]Th. Fauster, R. Schneider, H. Dürr, G. Engelmann, and E. Taglauer, Surf. Sci. **189/190**, 610 (1987).

[14]S. G. J. Mochrie, Phys. Rev. Lett. **59**, 304 (1987).

[15]B. M. Ocko and S. G. J. Mochrie, Phys. Rev. B **38**, 7378 (1988).

[16]P. Zeppenfeld, K. Kern, R. David, and G. Comsa, Phys. Rev. Lett. **62**, 63 (1989).

[17]G. Armand and P. Zeppenfeld, Phys. Rev. B **40**, 5936 (1989).

[18]S. Thevuthasan and W. N. Unertl, Appl. Phys. A **51**, 216 (1990).

[19]H. Dürr, R. Schneider, and Th. Fauster, Phys. Rev. B **43**, 12 187 (1990).

[20]A. P. Baddorf and E. W. Plummer, Phys. Rev. Lett. **66**, 2770 (1991).

[21]L. Yang and T. S. Rahman, Phys. Rev. Lett. **67**, 2327 (1991).

[22]B. Loisel, J. Lapujoulade, and V. Pontikis, Surf. Sci. **256**, 242 (1991).

[23]P. D. Ditlevsen, P. Stoltze, and J. K. Nørskov, Phys. Rev. B **44**, 13 002 (1991).

[24]H. Häkkinen and M. Manninen, Phys. Rev. B **46**, 1725 (1992); H. Häkkinen, J. Merikoski, M. Manninen, J. Timonen, and K. Kaski, Phys. Rev. Lett. **70**, 2451 (1993).

[25]K. Kern, in *Surface X-Ray and Neutron Scattering,* edited by H. Zabel and I. K. Robinson (Springer, Berlin, 1992), p. 69; K. Kern (unpublished).

[26]D. Gibbs, B. M. Ocko, D. M. Zehner, and S. G. J. Mochrie, Phys. Rev. B **38**, 7303 (1988).

[27]The Fresnel coefficient is given by $T(\theta)=2\sin\theta/\sin\theta+\sqrt{n^2-\cos^2\theta}$, where n is the complex index of refraction. In this experiment $T(\theta)$ is close to 1 for most values of H. Also, the polarization factor is a constant $P\approx 0.9$.

[28]C. J. Martin and D. A. O'Connor, J. Phys. C **10**, 3521 (1977).

[29]D. L. Adams, H. B. Nielsen, J. N. Andersen, I. Stensgaard, R. Feidenhans'l, and J. E. Sørensen, Phys. Rev. Lett. **49**, 669 (1982).

[30]H. L. Davis and J. R. Noonan, Surf. Sci. **126**, 245 (1983).

[31]D. L. Adams, H. B. Nielsen, and J. N. Andersen, Surf. Sci. **128**, 294 (1983).

[32]I. Stensgaard, R. Feidenhans'l, and J. E. Sørensen, Surf. Sci. **128**, 281 (1983).

[33]M. Copel, T. Gustafsson, W. R. Graham, and S. M. Yalisove, Phys. Rev. B **33**, 8110 (1986).

[34]F. A. Lindemann, Z. Phys. **11**, 609 (1910).